HHS Public Access

Author manuscript

J Am Chem Soc. Author manuscript; available in PMC 2022 August 23.

Published in final edited form as:

J Am Chem Soc. 2020 December 09; 142(49): 20536–20541. doi:10.1021/jacs.0c09753.

Rationally Designed Redox-Active Au(I) N-Heterocyclic Carbene: An Immunogenic Cell Death Inducer

Sajal Sen,
Department of Chemistry, The University of Texas at Austin, Austin, Texas 78712, United States

Stephanie Hufnagel,
College of Pharmacy, University of Texas at Austin, Austin, Texas 78712, United States

Esther Y. Maier,
Drug Dynamics Institute, College of Pharmacy, The University of Texas at Austin, Austin, Texas 78723, United States

Isaiah Aguilar,
Department of Chemistry, The University of Texas at Austin, Austin, Texas 78712, United States

Jayaraman Selvakumar,
Department of Chemistry, Wright State University, Dayton, Ohio 45435, United States

Jennie E. DeVore,
Drug Dynamics Institute, College of Pharmacy, The University of Texas at Austin, Austin, Texas 78723, United States

Vincent M. Lynch,
Department of Chemistry, The University of Texas at Austin, Austin, Texas 78712, United States

Kuppuswamy Arumugam,
Department of Chemistry, Wright State University, Dayton, Ohio 45435, United States

Zhengrong Cui,
College of Pharmacy, University of Texas at Austin, Austin, Texas 78712, United States

Jonathan L. Sessler,
Department of Chemistry, The University of Texas at Austin, Austin, Texas 78712, United States

Jonathan F. Arambula
Department of Chemistry, The University of Texas at Austin, Austin, Texas 78712, United States

Corresponding Authors zhengrong.cui@austin.utexas.edu, sessler@mail.utexas.edu, jfarambula@cm.utexas.edu.

ASSOCIATED CONTENT

Supporting Information

The Supporting Information is available free of charge at https://pubs.acs.org/doi/10.1021/jacs.0c09753.

Materials and methods, synthesis details, crystallographic data, electrochemical studies, biological assays, NMR spectra, and HRMS data (PDF)

Crystallographic data for **1** (CCDC 1951804) (CIF)

Crystallographic data for NQ-IPrAu-acetonyl (CCDC 1951803) (CIF)

The authors declare no competing financial interest.

Complete contact information is available at: https://pubs.acs.org/10.1021/jacs.0c09753

Abstract

Immunogenic cell death (ICD) is a way of reengaging the tumor-specific immune system. ICD can be induced by treatment with chemotherapeutics. However, only a limited number of drugs and other treatment modalities have been shown to elicit the biomarker responses characteristic of ICD and to provide an anticancer benefit in vivo. Here, we report a rationally designed redox-active Au(I) bis-N-heterocyclic carbene that induces ICD both in vitro and in vivo. This work benefits from a synthetic pathway that allows for the facile preparation of asymmetric redox-active Au(I) bis-N-heterocyclic carbenes.

Recent decades have borne witness to a paradigm shift in cancer care wherein the immune system is exploited to control and eradicate tumors.[1–3] These benefits have been propelled by a better comprehension of cancer biology and have spawned important discoveries involving targeted therapy.[4–6] Traditionally, cancer chemotherapeutics were thought to suppress the immune system.[7,8] However, recent studies have shown that certain anticancer drugs stimulate tumor-specific immune responses and reinstate immunosurveillance.[9] Immunogenic cell death (ICD) is a unique cell death mechanism, by which rejuvenation of the tumor-specific immune system occurs after treatment with certain therapeutic modalities.[10–13] Anticancer agents that induce ICD are expected to provide important complements to immune checkpoint inhibitors and may emerge as mainstays of cancer treatment in the years to come. Unfortunately, fewer than 1% of known anticancer agents have been documented as inducing ICD; thus, developing small molecules that elicit ICD would address a critical need.[14]

The concept of ICD was established in 2005 upon observation of tumor regression and effective treatment of mice injected with tumor cells that were pretreated in vitro with doxorubicin.[7] Recently, several platinum,[15–22] ruthenium,[23] and copper[24] complexes were reported as potential ICD inducers. ICD inducers are categorized into Type I and Type II. Type I inducers trigger ICD through endoplasmic reticulum (ER) stress via off-target secondary mechanisms, whereas Type II inducers trigger ICD directly via reactive oxygen species (ROS)-mediated ER stress and are generally more efficient.[25] Gold complexes, although studied for their antitumor potential, have not to our knowledge been investigated as potential ICD inducers.[26] Here, we report a rationally designed gold complex (**1**; Figure 1) that exhibits characteristic signatures of ICD induction in cancer cells and which inhibits tumor establishment in a mouse model under initial inoculation followed by cancer challenge conditions. We believe our strategy provides a new approach to the design of ICD inducers that promote tumor apoptosis and stimulate a tumor cell-specific immune response.[27–29]

Currently, structure–activity relationships that can guide the design of new ICD agents are lacking. We postulated that dual targeting of the cancer antioxidant network and promotion of ER stress could provide a rational approach to ICD induction. In this context, redox-active N-heterocyclic carbene (NHC) gold(I) complexes appeared attractive. The antitumor activity of cationic Au(I) bis-NHC complexes stems primarily from their selective interaction with the selenium-containing enzyme, thioredoxin reductase 2 (TrxR2), in mitochondria.[29,30] However, the resiliency of the highly networked antioxidant pathway

prevents effective tumor growth inhibition in vivo when only TrxR2 is targeted.[31] To overcome this limitation, we recently reported novel redox-active Au(I) bis-N-heterocyclic carbenes, containing ferrocene or quinone moieties appended to the NHC, exhibiting a dual mode of action against the cancer antioxidant network.[32,33] These complexes display anticancer activity in vitro as the result of combining TrxR2 inhibition (leading to a reduction in biological antioxidants) with increased oxidative stress (via redox cycling). These biochemical processes contribute to ROS generation and mitochondrial and ER stress in cancer cells,[32,33] which is a known prerequisite for ICD induction.[25] As detailed below, we have now found that the redox-active Au(I) bis-NHC (**1**) promotes ICD in vitro and in vivo as inferred from immunization experiments.

Figure 1 summarizes the preparation of complex **1**. In brief, NQ-IPrAu-Cl[34] was converted into the redox-active ketonyl complex NQ-IPrAu-acetonyl (for details, see the Supporting Information). Reaction of NQ-IPrAu-acetonyl with a hydroxyethyl imidazolium derivative gave **1** in 71% yield. This protocol provides an approach to asymmetric redox-active Au(I) bis-NHC complexes. X-ray diffraction quality single crystals of NQ-IPrAu-acetonyl and **1** were grown via slow diffusion of diethyl ether into saturated dichloromethane solutions of the respective complexes (Figures 1B and S1). The redox features of **1** were probed via cyclic and differential pulse voltammetry (DPV) (cf. Supporting Information). Half-wave reduction potentials for NQ-IPrAu-acetonyl and **1**, obtained from DPV measurements, are summarized (Table S2, Figures S6 and S7). According to the literature,[35–37] the redox potential of **1** makes it thermodynamically competent to accept electrons from electron-rich species such as NADH present in cells. The associated reduction leads to production of the semiquinone radical form, which undergoes autoxidation to regenerate the initial quinone with concomitant formation of ROS.

Several naphthoquinone-containing redox-active gold(I)-NHC complexes have been shown to induce apoptosis in cancer cells via two different modes of action (ROS level accentuation and a decrease in TrxR redox cycling-based ROS deactivation).[32] These features were expected to be recapitulated in the case of **1**. In fact, low IC_{50} values (Table 1) were observed against three test cell lines (A549 (human lung cancer), CT26 (mouse colon carcinoma), and HCT116 (human colon cancer)) 72 h post treatment as inferred from standard 3-(4,5-dimethylthiazol-2-yl)-2,5-diphenyltetrazolium bromide (MTT) assays (Figures S8–S10). Under analogous conditions, auranofin, an FDA-approved Au(I) complex known to exhibit antiproliferative activity, exerts weaker cytotoxicity (cf. Table 1).

Evidence for ROS generation came from confocal microscopic studies using A549 cells treated with 1.6 μM of **1** along with the ROS marker CM-H_2DCFDA. From that study, it was inferred that cells treated with **1** give rise to a marked increase in intracellular ROS levels compared to cells treated with vehicle alone (Figure 2). Furthermore, merged images involving coincubation with Mitotracker Red and the Hoechst stain revealed mitochondria to be the subcellular site of ROS accentuation. To quantify the increase in ROS levels, flow cytometric studies were carried out where A549 and CT26 cells were treated with **1** and auranofin in a dose-dependent manner. A significant increase in ROS level was observed in the case of both A549 and CT26 cells treated with **1** as compared to those treated with auranofin (Figures S11 and S12). Flow cytometry studies with annexin-V staining were

also carried out on CT26 cells; these revealed a dose-dependent increase in apoptotic cell death 4 h post incubation with **1** (Figure S13).[32] Redox-active Au(I) bis-NHC complexes have previously been reported to upregulate genes responsible for ER stress.[33] This coupled with the finding that incubation with **1** leads to increased intracellular ROS levels led us to suggest that it would act as a type II ICD inducer.[25] Evidence in support of this contention is provided below.

ICD can be characterized by three main biochemical hallmarks or damage-associated molecular patterns (DAMPs):[10,38,39] (i) relocation of the ER-resident chaperon protein calreticulin (CRT) to the outer cell membrane of early apoptotic cells ("eat me" signal), (ii) autophagy-dependent active secretion of adenosine triphosphate (ATP) as a result of apoptosis ("find me" signal) and, (iii) extracellular secretion of high mobility group box 1 (HMGB1) protein as a result of cell membrane permeabilization during late-stage apoptosis ("danger" signal). When observed in concert, these DAMPs are considered indicative of ICD induction in vitro.

We first tested whether **1** would promote CRT translocation via confocal microscopy. As inferred from the merged images, colocalization of emission signals from CRT antibody with the cell membrane immunostaining wheat-germ agglutinin (WGA) antibody suggests CRT translocation to the cell membrane occurs upon incubation with **1** (Figure 3A). To quantify the CRT translocation, dose dependent flow cytometry studies were performed on nonpermeabilized CT26 cells. Cells undergoing early apoptosis showed a significant level of CRT release after treatment with **1** at 2.5 μM for 24 h (Figure S14 and Figure 3B). Oxaliplatin, a known ICD inducer,[15,16] was also included as a control for comparison. Importantly, cells treated with 2.5 μM of **1** displayed cell membrane CRT translocation to a similar level as cells treated with 300 μM of oxaliplatin.

Next, we assessed the release of ATP in CT26 cells in the presence of **1** and compared it with oxaliplatin (Figure 3C and Figure S15). The amount of released ATP in supernatants 1 h and 4 h post-treatment of both complexes was measured using a luciferin-based assay. Complex **1** at 5 μM was found to be effective in inducing ATP secretion at a level analogous to that produced by 150 μM of oxaliplatin, as determined 4 h post-treatment (Figure 3C). Finally, an ELISA assay was performed (Figure 3D) to determine whether incubation with **1** led to the presence of HMGB1 in the supernatant of treated CT26 cells. Again, **1** proved more effective than oxaliplatin, as determined 4 h post-treatment. Considered in concert, these findings prompted us to test the activity of **1** in vivo. Such tests were deemed necessary because a number of anticancer agents or therapies are known to trigger ICD-associated biomarkers in vitro but have yet to show antitumor immunity effects in vivo.[16,23,24] However, in the absence of demonstrated tumor establishment inhibition when an animal is subject to a tumor challenge, the promise of these species as ICD inducers remains uncertain.[23,25]

To test whether **1** could be used to promote ICD-mediated tumor eradication in vivo, studies on syngeneic immunocompetent mice were performed (Figure 4A). Oxaliplatin, which has been shown to elicit ICD in several rodent models of colon cancer,[15] was used as a positive control. In a first study, a group of BALB/c mice (n = 10; data are pooled from two

independent repeat experiments with $n = 5$ each) were subcutaneously injected on the right flank with CT26 cells (3×10^6) that were pretreated with varying concentrations (5, 10, or 100 μM) of **1** or 150 μM of oxaliplatin for 4 h (to induce the desired ICD biomarkers and create a potential anticancer immune response). Untreated CT26 cells subjected to three freeze–thaw cycles to induce necrosis were injected as a negative control. Seven days later, the mice were challenged subcutaneously in the left flank with naıve, live CT26 cells (5×10^5), and the tumor growth was monitored over time. All mice treated with freeze–thawed CT26 cells developed measurable tumors on the left (challenge) flank after 6 days, whereas some mice implanted with CT26 cells pretreated with **1** at 5, 10, or 100 μM or oxaliplatin at 150 μM experienced delayed or no tumor development. This delay was found to be statistically significant in all groups except the group involving 100 μM of **1** (Figure 4B), where it is assumed the high levels of initial cytotoxicity precluded an ICD response. While these data provide support for our initial hypothesis that **1** would prove effective at inducing ICD, it should be noted that for both **1** (at 5 and 10 μM doses) and oxaliplatin, drug-treated tumor cell inoculation resulted in tumor growth (Figure S16) on the original treatment flank (i.e., the right flank). Due to this, the study was ended early.

To overcome the limitations associated with growth of the original tumor, an in vivo strategy was developed that involved resecting the initial treatment (right flank) tumors before they reached 200 mm^3 in size (Figure 4A). This allowed us to determine the potential of both **1** and oxaliplatin to induce an immune response and effect tumor-growth inhibition (challenge flank). Also, this strategy provides a test of whether the presumed ICD-induced immune response would remain active even after removal of the original drug-treated tumor. As in the initial study, the benefits of **1** were not apparent at the highest 100 μM dose level. However, for the CT26 tumor cells treated with **1** at 5 and 10 μM doses, the development of the challenge tumors was inhibited relative to the group treated with only freeze–thawed cells (Figure 4C). This result continued 42 days postchallenge. The data also revealed that CT26 cells treated with **1** at 10 μM were more effective at delaying challenge tumor growth than oxaliplatin used at a much higher dose (150 μM; 15× higher). These in vivo studies thus support the notion that **1** induces CT26 tumor cells to undergo ICD and that pretreatment of tumor cells resulted in inhibiting or delaying the growth of tumors on the challenge flank.

In summary, the rationally designed Au(I) bis-NHC complex **1** proved to be efficacious as an ICD inducer. Its efficacy in triggering ICD is ascribed to its ability to target the cancer antioxidant network via two modes of action. We believe this work highlights a new approach to preparing ICD inducers that involves controlling oxidative and ER stress via redox modulation. This work also highlights a novel strategy that can be used to prepare asymmetric redox-active Au(I) bis-NHC complexes. This should allow ready access to a library of redox-active Au(I) bis-NHC complexes and permit detailed explorations of structure–activity relationships as they relate to ICD induction. Studies along these lines are in progress.

Supplementary Material

Refer to Web version on PubMed Central for supplementary material.

ACKNOWLEDGMENTS

Partial funding from the National Institutes of Health National Cancer Institute (R01 CA68682 to J.L.S., R01 CA135274 to Z.C., and R15 CA232765 to J.F.A. and K.A.) is acknowledged, as is support from the Robert A. Welch Foundation (F-0018, J.L.S.).

REFERENCES

(1). Farkona S; Diamandis EP; Blasutig IM Cancer Immunotherapy: The Beginning of the End of Cancer? BMC Med. 2016, 14 (1), 1–18. [PubMed: 26728489]

(2). Sharma P; Allison JP Immune Checkpoint Targeting in Cancer Therapy: Toward Combination Strategies with Curative Potential. Cell 2015, 161 (2), 205–214. [PubMed: 25860605]

(3). Iams WT; Porter J; Horn L. Immunotherapeutic Approaches for Small-Cell Lung Cancer. Nat. Rev. Clin. Oncol 2020, 17 (5), 300–312. [PubMed: 32055013]

(4). Lee YT; Tan YJ; Oon CE Molecular Targeted Therapy: Treating Cancer with Specificity. Eur. J. Pharmacol 2018, 834, 188–196. [PubMed: 30031797]

(5). Tsimberidou AM Targeted Therapy in Cancer. Cancer Chemother. Pharmacol 2015, 76 (6), 1113–1132. [PubMed: 26391154]

(6). Chae YK; Pan AP; Davis AA; Patel SP; Carneiro BA; Kurzrock R; Giles FJ Path toward Precision Oncology: Review of Targeted Therapy Studies and Tools to Aid in Defining “Actionability” of a Molecular Lesion and Patient Management Support. Mol. Cancer Ther 2017, 16 (12), 2645–2655. [PubMed: 29203694]

(7). Casares N; Pequignot MO; Tesniere A; Ghiringhelli F; Roux S; Chaput N; Schmitt E; Hamai A; Hervas-Stubbs S; Obeid M; Coutant F; Metivier D; Pichard E; Aucouturier P; Pierron G; Garrido C; Zitvogel L; Kroemer G. Caspase-Dependent Immunogenicity of Doxorubicin-Induced Tumor Cell Death. J. Exp. Med 2005, 202 (12), 1691–1701. [PubMed: 16365148]

(8). Cheson BD Infectious and Immunosuppressive Complications of Purine Analog Therapy. J. Clin. Oncol 1995, 13 (9), 2431–2448. [PubMed: 7666104]

(9). Zitvogel L; Galluzzi L; Smyth MJ; Kroemer G. Mechanism of Action of Conventional and Targeted Anticancer Therapies: Reinstating Immunosurveillance. Immunity 2013, 39 (1), 74–88. [PubMed: 23890065]

(10). Krysko DV; Garg AD; Kaczmarek A; Krysko O; Agostinis P; Vandenabeele P. Immunogenic Cell Death and DAMPs in Cancer Therapy. Nat. Rev. Cancer 2012, 12 (12), 860–875. [PubMed: 23151605]

(11). Kroemer G; Galluzzi L; Kepp O; Zitvogel L. Immunogenic Cell Death in Cancer Therapy. Annu. Rev. Immunol 2013, 31 (1), 51–72. [PubMed: 23157435]

(12). Englinger B; Pirker C; Heffeter P; Terenzi A; Kowol CR; Keppler BK; Berger W. Metal Drugs and the Anticancer Immune Response. Chem. Rev 2019, 119 (2), 1519–1624. [PubMed: 30489072]

(13). Inoue H; Tani K. Multimodal Immunogenic Cancer Cell Death as a Consequence of Anticancer Cytotoxic Treatments. Cell Death Differ. 2014, 21 (1), 39–49. [PubMed: 23832118]

(14). Kepp O; Senovilla L; Kroemer G. Immunogenic Cell Death Inducers as Anticancer Agents. Oncotarget 2014, 5 (14), 5190–5191. [PubMed: 25114034]

(15). Tesniere A; Schlemmer F; Boige V; Kepp O; Martins I; Ghiringhelli F; Aymeric L; Michaud M; Apetoh L; Barault L; Mendiboure J; Pignon J-P; Jooste, V; van Endert, P; Ducreux, M; Zitvogel, L; Piard, F; Kroemer, G Immunogenic Death of Colon Cancer Cells Treated with Oxaliplatin. Oncogene 2010, 29 (4), 482–491. [PubMed: 19881547]

(16). Wong DYQ; Ong WWF; Ang WH Induction of Immunogenic Cell Death by Chemotherapeutic Platinum Complexes. Angew. Chem., Int. Ed 2015, 54 (22), 6483–6487.

(17). Huang K-B; Wang F-Y; Feng H-W; Luo H; Long Y; Zou T; Chan ASC; Liu R; Zou H; Chen Z-F; Liu Y-C; Liu Y-N; Liang H. An Aminophosphonate Ester Ligand-Containing Platinum(II) Complex Induces Potent Immunogenic Cell Death: In Vitro and Elicits Effective Anti-Tumour Immune Responses in Vivo. Chem. Commun 2019, 55 (87), 13066–13069.

(18). Sabbatini M; Zanellato I; Ravera M; Gabano E; Perin E; Rangone B; Osella D. Pt(IV) Bifunctional Prodrug Containing 2-(2-Propynyl)Octanoato Axial Ligand: Induction of Immunogenic Cell Death on Colon Cancer A. J. Med. Chem 2019, 62 (7), 3395–3406. [PubMed: 30879295]

(19). Tang L; Cai D; Qin M; Lu S; Hu MH; Ruan S; Jin G; Wang Z. Oxaliplatin-Based Platinum(IV) Prodrug Bearing Toll-like Receptor 7 Agonist for Enhanced Immunochemotherapy. ACS Omega 2020, 5 (1), 726–734. [PubMed: 31956823]

(20). Tham MJR; Babak MV; Ang WH PlatinER: A Highly Potent Anticancer Platinum(II) Complex That Induces Endoplasmic Reticulum Stress Driven Immunogenic Cell Death. Angew. Chem., Int. Ed 2020, 59 (43), 19070–19078.

(21). Novohradsky V; Pracharova J; Kasparkova J; Imberti C; Bridgewater HE; Sadler PJ; Brabec V. Induction of Immunogenic Cell Death in Cancer Cells by a Photoactivated Platinum(IV) Prodrug. Inorg. Chem. Front 2020, 7, 4150–4159. [PubMed: 34540235]

(22). Yamazaki T; Buqué A; Ames TD; Galluzzi L. PT-112 Induces Immunogenic Cell Death and Synergizes with Immune Checkpoint Blockers in Mouse Tumor Models. Oncoimmunology 2020, 9 (1), 1721810.

(23). Wernitznig D; Kiakos K; Del Favero G; Harrer N; MacHat H; Osswald A; Jakupec MA; Wernitznig A; Sommergruber W; Keppler BK First-in-Class Ruthenium Anticancer Drug (KP1339/IT-139) Induces an Immunogenic Cell Death Signature in Colorectal Spheroids: In Vitro. Metallomics 2019, 11 (6), 1044–1048. [PubMed: 30942231]

(24). Kaur P; Johnson A; Northcote-Smith J; Lu C; Suntharalingam K. Immunogenic Cell Death of Breast Cancer Stem Cells by an Endoplasmic Reticulum-Targeting Copper(II) Complex. ChemBioChem 2020, 21, 1–8.

(25). Garg AD; Dudek-Peric AM; Romano E; Agostinis P. Immunogenic Cell Death. Int. J. Dev. Biol 2015, 59 (1–3), 131–140. [PubMed: 26374534]

(26). Yue S; Luo M; Liu H; Wei S. Recent Advances of Gold Compounds in Anticancer Immunity. Front. Chem 2020, 8 (543), 1–14. [PubMed: 32117862]

(27). Berners-Price SJ; Filipovska A. Gold Compounds as Therapeutic Agents for Human Diseases. Metallomics 2011, 3 (9), 863–873. [PubMed: 21755088]

(28). Hickey JL; Ruhayel RA; Barnard PJ; Baker MV; Berners-Price SJ; Filipovska A. Mitochondria-Targeted Chemotherapeutics: The Rational Design of Gold(I) N-Heterocyclic Carbene Complexes That Are Selectively Toxic to Cancer Cells and Target Protein Selenols in Preference to Thiols. J. Am. Chem. Soc 2008, 130 (38), 12570–12571. [PubMed: 18729360]

(29). Sen S; Li Y; Lynch V; Arumugam K; Sessler JL; Arambula JF Expanding the Biological Utility of Bis-NHC Gold(i) Complexes through Post Synthetic Carbamate Conjugation. Chem. Commun 2019, 55 (71), 10627–10630.

(30). Sen S; Perrin MW; Sedgwick AC; Dunsky EY; Lynch VM; He X; Sessler JL; Arambula JF Toward Multifunctional Anticancer Therapeutics: Post-Synthetic Carbonate Functionalisation of Asymmetric Au(I) Bis-N-Heterocyclic Carbenes. Chem. Commun 2020, 56 (57), 7877–7880.

(31). Eriksson SE; Prast-Nielsen S; Flaberg E; Szekely L; Arnér ESJ High Levels of Thioredoxin Reductase 1 Modulate Drug-Specific Cytotoxic Efficacy. Free Radical Biol. Med 2009, 47 (11), 1661–1671. [PubMed: 19766715]

(32). Arambula JF; McCall R; Sidoran KJ; Magda D; Mitchell NA; Bielawski CW; Lynch VM; Sessler JL; Arumugam K. Targeting Antioxidant Pathways with Ferrocenylated N-Heterocyclic Carbene Supported Gold(I) Complexes in A549 Lung Cancer Cells. Chem. Sci 2017, 7, 1245–1256.

(33). McCall R; Miles M; Lascuna P; Burney B; Patel Z; Sidoran KJ; Sittaramane V; Kocerha J; Grossie DA; Sessler JL; Arumugam K; Arambula JF Dual Targeting of the Cancer Antioxidant Network with 1,4-Naphthoquinone Fused Gold(I) N-Heterocyclic Carbene Complexes. Chem. Sci 2017, 8, 5918–5929. [PubMed: 29619196]

(34). Michalska M; Grudzién K; Małecki P; Grela K. Gold(I)-Catalyzed Formation of Naphthalene/Acenaphthene Heterocyclic Acetals. Org. Lett 2018, 20 (4), 954–957. [PubMed: 29412677]

(35). Gopinath P; Mahammed A; Ohayon S; Gross Z; Brik A. Understanding and Predicting the Potency of ROS-Based Enzyme Inhibitors, Exemplified by Naphthoquinones and Ubiquitin Specific Protease-2. Chem. Sci 2016, 7 (12), 7079–7086. [PubMed: 28451143]

(36). Davies KJA; Doroshow JH; Hochstein P. Mitochondrial NADH Dehydrogenase-Catalyzed Oxygen Radical Production by Adriamycin, and the Relative Inactivity of 5-Iminodaunorubicin. FEBS Lett. 1983, 153 (1), 227–230. [PubMed: 6298008]

(37). Klotz LO; Hou X; Jacob C. 1,4-Naphthoquinones: From Oxidative Damage to Cellular and Inter-Cellular Signaling. Molecules 2014, 19 (9), 14902–14918. [PubMed: 25232709]

(38). Kroemer G; Galluzzi L; Kepp O; Zitvogel L. Immunogenic Cell Death in Cancer Therapy. Annu. Rev. Immunol 2013, 31 (1), 51–72. [PubMed: 23157435]

(39). Terenzi A; Pirker C; Keppler BK; Berger W. Anticancer Metal Drugs and Immunogenic Cell Death. J. Inorg. Biochem 2016, 165, 71–79. [PubMed: 27350082]

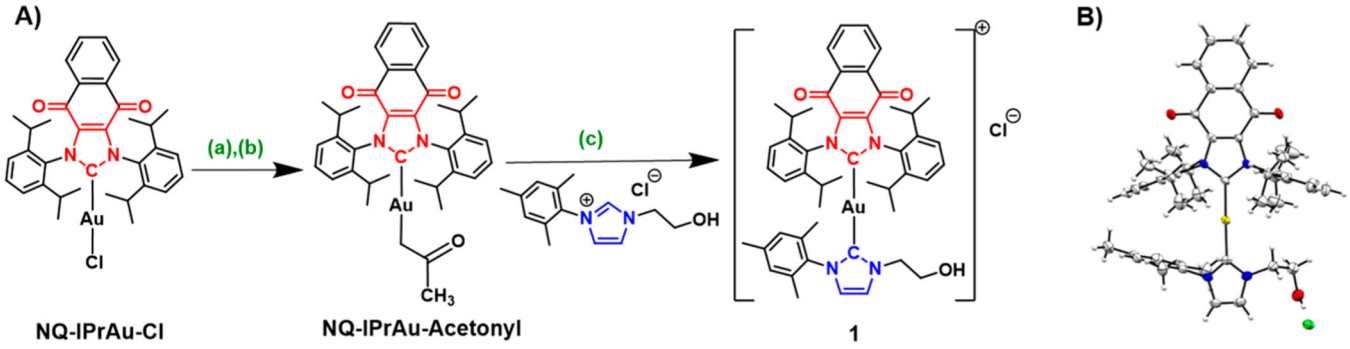

Figure 1.

(A) Synthetic scheme for **1**. (a) NaOH (7.5 equiv), *t*-amyl alcohol (cat.), *t*-butyl alcohol (cat.), THF, RT, 24 h. (b) Acetone, RT, 4 h. c) toluene, 90 °C, 24 h. (B) ORTEP representation of **1** rendered using POV-Ray. Thermal ellipsoids are at the 50% probability level.

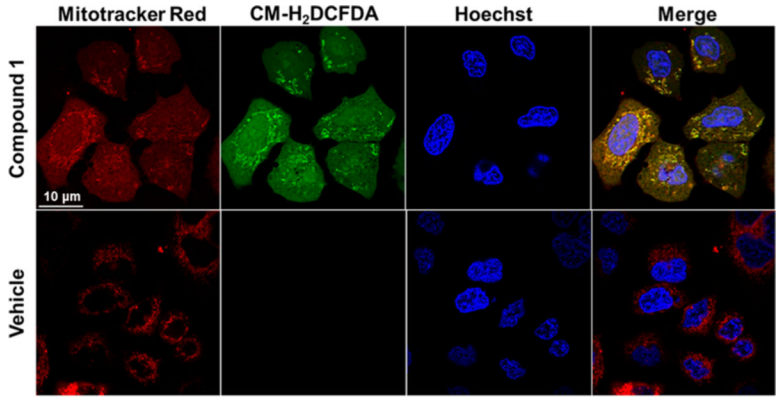

Figure 2.

Confocal microscopy images showing ROS generation in A549 cells 4 h post treatment with 1.6 μM of **1**. In the case of **1**, the merged image of Mitotracker Red and CM-H_2DCFDA provides evidence for ROS production in the mitochondria.

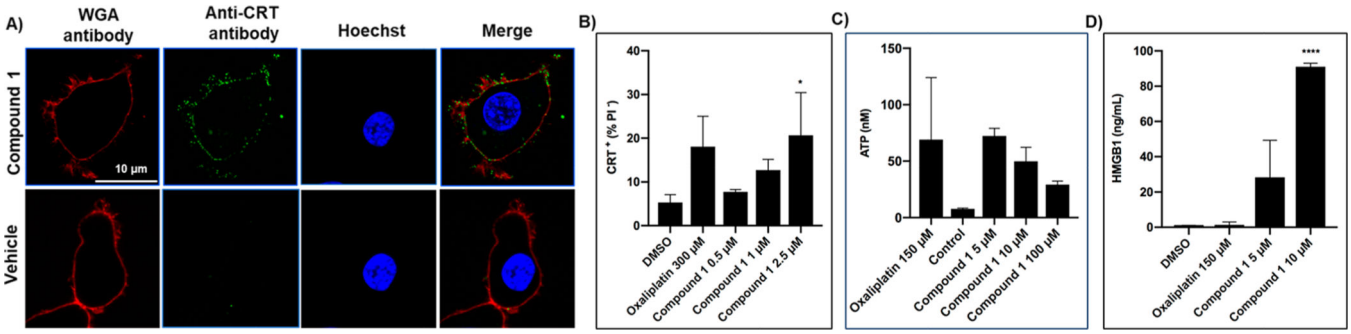

Figure 3.

(A) Confocal microscopy images showing calreticulin (CRT) translocation in CT26 cells 4 h post-treatment with 5 μM of **1**. No CRT release was seen in the case of vehicle alone. (B) Flow cytometry showing dose dependent CRT release in CT26 cells 24 h post treatment with **1** or oxaliplatin. (C) Dose dependent ATP release in CT26 cells 4 h post-treatment with **1** or oxaliplatin. (D) Dose dependent release of HMGB1 protein in CT26 cells 4 h post-treatment with **1** or oxaliplatin (one-way ANOVA with Tukey's multiple comparison). Data are mean ± SD and $p < 0.05$ is significant. *$p < 0.05$, **$p < 0.01$, ***$p < 0.001$, ****$p < 0.0001$).

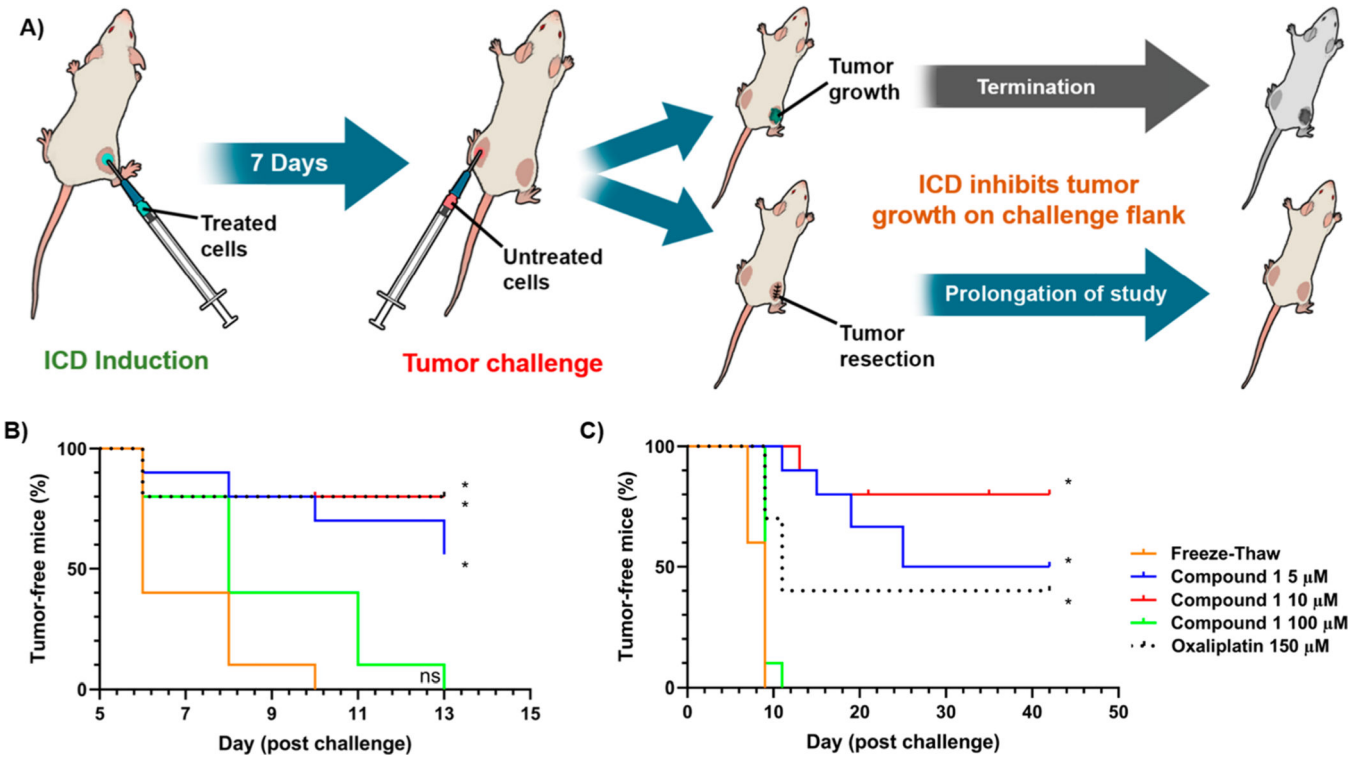

Figure 4.

(A) Schematic diagram illustrating in vivo strategies. (B) Percent tumor-free mice (i.e., left flank tumor) injected with pretreated CT26 cells with varying doses of 1 or 150 μM oxaliplatin in the right flank and then inoculated (i.e., challenged) with CT26 cells in the left flank when right flank tumors were not resected ($n = 10$, data were combined from two independent experiments). (C) Percent tumor-free mice (i.e., left flank tumor) when right flank tumors were resected before they reached >200 mm^3 in size. Mice ($n = 10$) were censored (i.e., removed from the study) if they reached an end point for euthanasia before developing a left flank tumor (for details, see Supporting Information). (Mantel-Cox Log-rank test, $p < 0.005$ (Bonferroni-corrected) was considered significant, * indicates difference from freeze–thaw.)

Table 1.

IC_{50} Values (μM) for 1 and Auranofin against Various Cancer Cells, as Inferred from 72 h MTT Assays

cell Lines	A549	HCT116	CT26
1	0.030 ± 0.001	0.030 ± 0.002	0.405 ± 0.007
auranofin	2.181 ± 0.147	1.348 ± 0.103	0.821 ± 0.030